Molecular Therapy
Oncology
Original Article

Enhancement of radio-sensitivity by inhibition of Janus kinase signaling with oclacitinib in canine tumor cell lines

Ryo Owaki,[1] Kenji Hosoya,[2] Tatsuya Deguchi,[2] Satoru Konnai,[3,4] Naoya Maekawa,[3] Tomohiro Okagawa,[3] Hironobu Yasui,[5] Sangho Kim,[1] Takafumi Sunaga,[1] and Masahiro Okumura[1]

[1]Laboratory of Veterinary Surgery, Department of Veterinary Clinical Sciences, Faculty of Veterinary Medicine, Hokkaido University, Sapporo, Japan; [2]Veterinary Teaching Hospital, Faculty of Veterinary Medicine, Hokkaido University, Sapporo, Japan; [3]Department of Advanced Pharmaceutics, Faculty of Veterinary Medicine, Hokkaido University, Sapporo, Japan; [4]Laboratory of Infectious Diseases, Department of Disease Control, Faculty of Veterinary Medicine, Hokkaido University, Sapporo, Japan; [5]Laboratory of Radiation Biology, Department of Applied Veterinary Science, Graduate School of Veterinary Medicine, Hokkaido University, Sapporo, Japan

A combination of irradiation and oclacitinib, a Janus kinase (JAK) inhibitor used in dogs, could lead to synergistic anti-cancer effects in canine tumors. However, the anti-tumor effects of oclacitinib remain unclear. This study investigated the radio-sensitizing effect of oclacitinib in canine tumors and determined its underlying mechanisms using osteosarcoma (HMPOS), malignant melanoma (CMeC), and thyroid adenocarcinoma (CTAC) cell lines. A clonogenic assay and a tumor growth assessment in a xenograft mouse model (BALB/cAJcl-nu/nu) were performed to evaluate the radio-sensitizing effects of oclacitinib. Oclacitinib enhanced the radio-sensitivity of tumor cells both *in vitro* and *in vivo*. The signal transducer and activator of transcription (STAT)3 expression was activated and suppressed by oclacitinib in X-irradiation-exposed cells. Oclacitinib enhanced radiation-induced apoptosis only in HMPOS cells by inhibiting anti-apoptotic genes. In addition, oclacitinib inhibited the transcription of cell-cycle-regulating genes and arrested cell cycle progression from the G1 phase to subsequent phases. In conclusion, oclacitinib enhanced radio-sensitivity both *in vitro* and *in vivo* by triggering apoptosis and impeding cell cycle progression via STAT3 inhibition in canine tumor cell lines. This study suggested the clinical therapeutic potential of oclacitinib and radiation therapy in enhancing treatment efficacy and outcomes in canine tumors.

INTRODUCTION

Radiation therapy is an effective treatment for local tumor control in canine tumor patients. However, its efficacy is often limited, with frequent local recurrences and metastases. Novel approaches are required to improve the outcomes of radiation therapy in canine cancer.

The Janus kinase (JAK) and signal transducer and activator of transcription (STAT) families play pivotal roles in mediating essential cell processes, such as hematopoiesis, cell proliferation, differentiation, and apoptosis.[1] After activation by JAK through the phosphorylation of a conserved tyrosine residue (Tyr 705), STAT translocates into the nucleus, regulating specific target gene transcription.[2,3] Specificity in this signaling pathway was determined by combining distinct JAK proteins (JAK1, JAK2, JAK3, and TYK2) and members of the STAT family (STAT1, STAT2, STAT3, STAT4, STAT5, and STAT6).[1]

Oclacitinib, an orally available JAK inhibitor, is a therapeutic agent for canine pruritus associated with atopic and allergic dermatitis.[4] It is safe for extended use in dogs aged 12 months or older.[5] Oclacitinib preferentially inhibits JAK1 over JAK2 at the recommended doses in the clinical setting. It suppresses the production of JAK1-dependent cytokines involved in allergy and inflammation, such as interleukin (IL)-2, IL-4, IL-6, and IL-13 with minimal effects on the production of JAK2-dependent cytokines associated with hematopoiesis (granulocyte-macrophage colony-stimulating factor and erythropoietin) in cell assays.[6]

Among the JAK-STAT signaling pathways, STAT3 is known to promote tumor growth. Persistent STAT3 activation correlates with tumor progression and poor prognosis in various human cancers, including breast cancer, prostate carcinoma, and osteosarcoma.[7–9] Several studies have demonstrated persistent STAT3 activation driven by factors such as G-protein-coupled receptors, non-receptor tyrosine kinases, and IL-6 family cytokines. Its activation inhibits apoptotic signals and promotes cell proliferation, angiogenesis, and immune evasion in various human tumor cell lines, including melanoma, prostate carcinoma, and osteosarcoma.[8,10–13] Persistent STAT3 activation has also been reported in several canine tumors, including osteosarcoma, B cell lymphoma, and malignant melanoma, and is correlated with poor tumor prognosis.[14–16] This activation

Received 6 November 2024; accepted 30 January 2025;
https://doi.org/10.1016/j.omton.2025.200946.

Correspondence: Kenji Hosoya, Veterinary Teaching Hospital, Faculty of Veterinary Medicine, Hokkaido University, Sapporo, Japan.
E-mail: hosoya@vetmed.hokudai.ac.jp

contributes to tumor angiogenesis and apoptosis suppression in canine osteosarcoma cell lines.[15,17] Consequently, inhibition of STAT3 signaling is a promising therapeutic approach for human and canine cancers.

Some studies have recently shown radiation-induced STAT3 phosphorylation through several mechanisms, such as secreted phosphoprotein 1-JAK2 signaling augmentation, epidermal growth factor receptor or IL-6 expression enhancement, and induction of Src phosphorylation. These processes ultimately promote tumor radioresistance by DNA damage repair and angiogenesis in several human cancer cells, including esophageal carcinoma and prostate cancer.[18–20] In contrast, the JAK inhibitors suppress persistent and radiation-induced STAT3 activation and enhance radio-sensitivity in several cancer cell lines by inhibiting programmed death ligand 1 expression and cell cycle progression and enhancing apoptosis.[21–23] In addition, combination treatment with irradiation and a JAK or STAT3 inhibitor has demonstrated radio-sensitizing effects in tumor xenograft mouse models.[22,24,25] Therefore, regulating aberrant and increased STAT3 activation could be an effective treatment for radio-resistant tumors, indicating the potential of oclacitinib as an anti-tumor agent by inhibiting STAT3 expression through JAK signaling blockade in canine tumors.

This study investigated the radio-sensitizing effects of oclacitinib and elucidated its underlying mechanisms *in vitro* and *in vivo* using canine tumor cell lines. The radio-sensitizing effect of oclacitinib was evaluated using a clonogenic assay and tumor growth in a xenograft mouse model. The protein levels of STAT3 and poly (ADP-ribose) polymerase (PARP) were assessed by western blotting. Gene transcript levels regulated by STAT3 were examined using quantitative reverse transcriptase PCR (RT-qPCR). Apoptosis and the cell cycle were analyzed using flow cytometry.

RESULTS

Induction of STAT3 activation in X-irradiated cells in a dose- and time-dependent manner

Western blotting was used to assess the alterations in STAT3 expression and phosphorylation by X-irradiation. At 24 h after exposure to 5 Gy X-irradiation, STAT3 activation was significantly induced and dose-dependently upregulated in HMPOS. Whereas STAT3 activation was similarly increased with 5 Gy X-irradiation in CMeC and 7.5 Gy in CTAC, no significant change was observed in 5–10 Gy X-irradiation in CMeC, and STAT3 activation decreased 10 Gy X-irradiation in CTAC (Figures 1A and 1B). Expression was significantly enhanced in a time-dependent manner in all tumor cell lines in cells exposed to 5 Gy X-irradiation (Figures 1C and 1D).

Radio-sensitizing effect of oclacitinib *in vitro* and its ability to inhibit STAT3 activation

To investigate the radio-sensitizing effects of oclacitinib, a clonogenic assay was performed. First, to test the cytotoxicity of oclacitinib, the cells were treated with various concentrations of oclacitinib for 24 h. Cell viability decreased after oclacitinib exposure in all tumor cell lines (Figure 2A). Therefore, 500 nM was chosen as the optimal oclacitinib concentration for subsequent experiments to maintain cell viability at acceptable levels (>60%) while maintaining an effective dose to exert the inhibitory activity in the cell culture. Next, colony survival in tumor cell lines was quantified after X-irradiation with 500 nM of oclacitinib. Oclacitinib significantly decreased colony formation in all tumor cell lines compared to the control (without oclacitinib) (Figure 2B). Western blotting confirmed the inhibitory effects of oclacitinib on STAT3 activation. Oclacitinib significantly suppressed X-irradiation-induced STAT3 activation in all tumor cell lines (Figures 3A and 3B).

Induction of apoptosis after X-irradiation and oclacitinib combination treatment

Western blotting analysis showed that PARP activation was significantly induced in cells treated with X-irradiation. The combination of X-irradiation and oclacitinib further enhanced PARP activation compared to the effect of X-irradiation alone in HMPOS but not in CMeC or CTAC (Figures 3A and 3C). To evaluate anti-apoptotic genes, the mRNA expression of *Survivin*, *B cell lymphoma-extra large* (*Bcl-x_L*), and *Myeloid leukemia 1* (*MCL1*) was analyzed using RT-qPCR. *Bcl-x_L* and *MCL1* expression in HMPOS and *Bcl-x_L* expression in CTAC was significantly suppressed in HMPOS treated with oclacitinib compared to cells without treatment. In addition, the expression of all the genes was significantly decreased in cells treated with the X-irradiation and oclacitinib combination compared with cells treated with X-irradiation alone. Although the same trend was observed for each treatment, differences in gene expression did not reach statistical significance in CMeC (Figure 4A). Next, cells stained with annexin V were designated as undergoing apoptosis. Annexin V staining was used to examine the apoptosis rate in cells treated with X-irradiation and oclacitinib. The proportion of apoptotic cells significantly increased in cells treated with X-irradiation alone and in combination with other treatments in all tumor cell lines. The proportion of apoptotic cells further increased in cells treated with the combination of treatments compared with cells treated with either oclacitinib or X-irradiation alone in HMPOS and CTAC but not in CMeC (Figure 5). Therefore, oclacitinib increased cell death induced by X-irradiation. The apoptotic cell rates in HMPOS, CMeC, and CTAC cells were 8.11% ± 0.6%, 4.95% ± 0.11%, and 3.15% ± 0.07% under control conditions; 18.07% ± 0.59%, 3.15% ± 0.05%, and 5.09% ± 0.13% after oclacitinib treatment; 18.11% ± 0.69%, 8.38% ± 0.11%, and 6.50% ± 0.19% after X-irradiation; and 27.53% ± 0.38%, 7.01% ± 0.46%, and 12.47% ± 0.19% after X-irradiation and oclacitinib treatment, respectively.

Inhibition of cell cycle progression from G1 to later phases by oclacitinib treatment

To evaluate cell-cycle-regulating genes, the mRNA expression of *CCND1*, *cyclin-dependent kinase* (*CDK*)*4*, and *CDK6* was analyzed using RT-qPCR. All gene expressions in HMPOS, all gene expressions except for *CCND1* in CMeC, and all gene expressions except for *CDK4* were significantly inhibited in cells treated with oclacitinib and the combination of X-irradiation and oclacitinib compared with untreated cells and cells treated with X-irradiation alone.

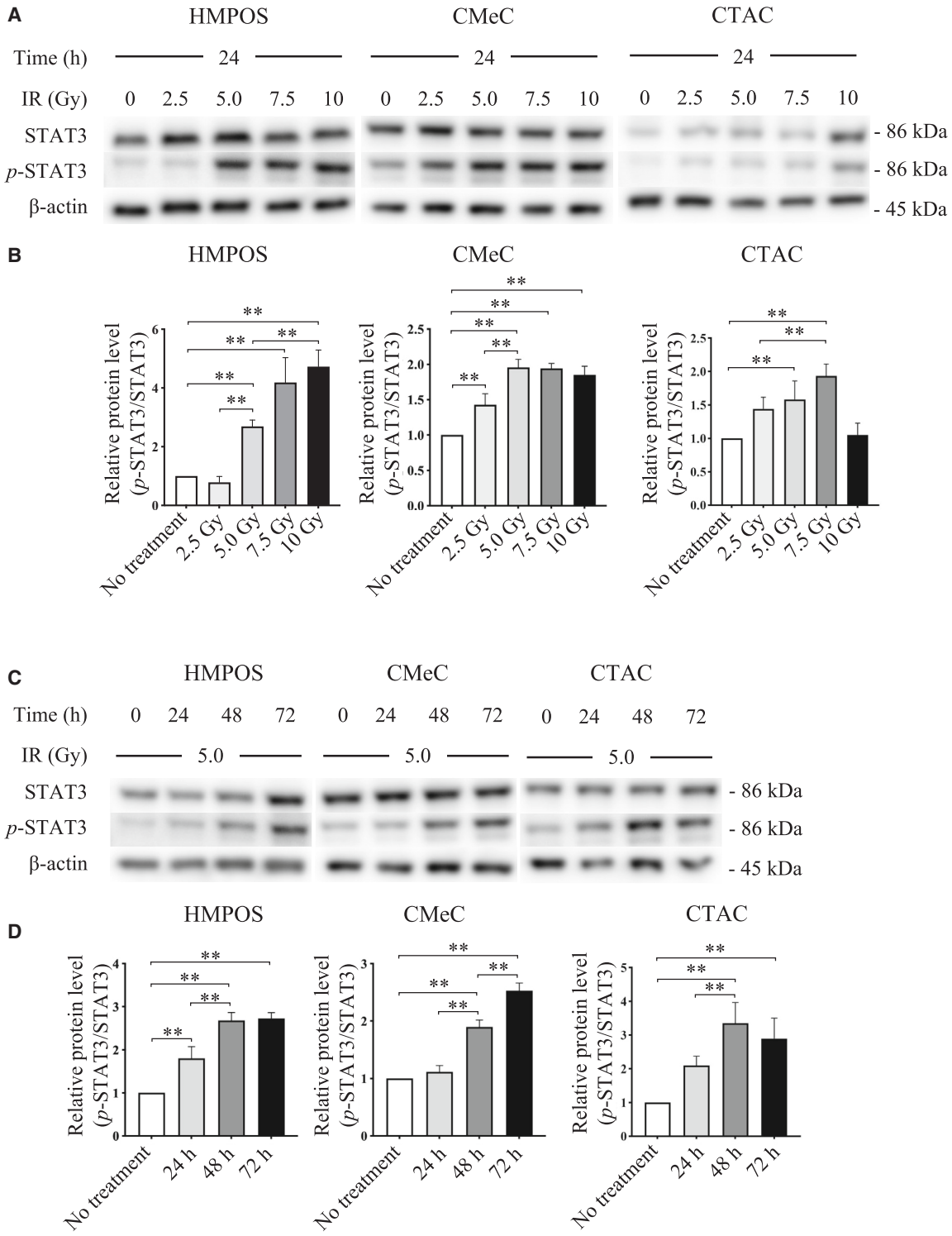

Figure 1. Induction of STAT3 protein activation in canine tumor cells exposed to X-irradiation, depending on dose and time

(A) Analysis of STAT3 and phosphorylated STAT3 (p-STAT3) expression in cells 24 h after 2.5–10 Gy X-irradiation (IR) using western blot. β-actin served as a reference protein. (B) Comparison of the expression level of p-STAT3 relative to the corresponding total proteins. (C) Analysis of STAT3 and p-STAT3 expression in cells 24−72 h following treatment with IR using western blot. β-actin served as a reference protein. (D) Comparison of the expression level of p-STAT3 relative to the corresponding total proteins. The error bars represent the SD of the mean calculated from three separate and independent experiments. Statistical significance was analyzed by Tukey's multiple comparison test. $^{**}p < 0.01$.

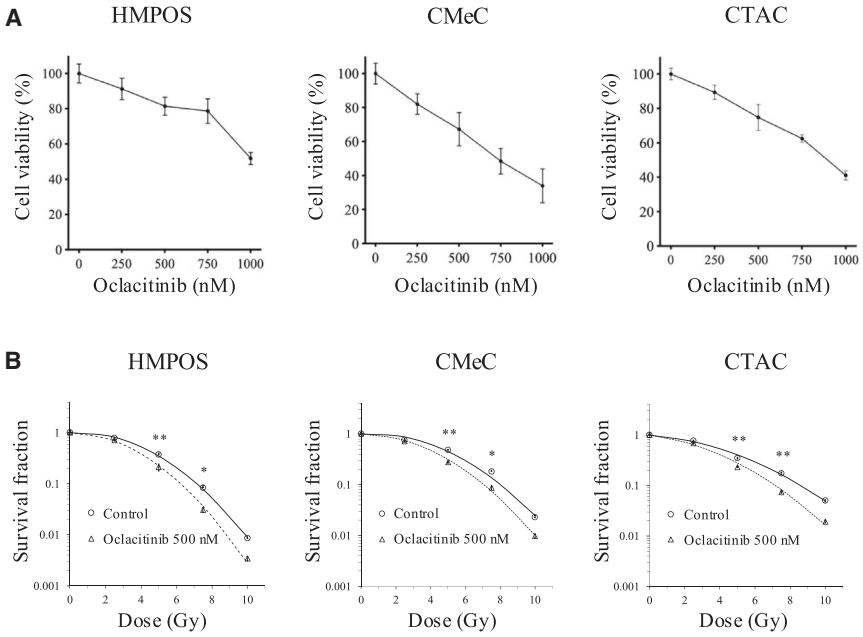

Figure 2. Radio-sensitizing effects by oclacitinib in canine tumor cell lines

(A) Cell viability following treatment with 250–1,000 nM of oclacitinib. (B) Survival curves of cell colonies after X-irradiation in cell cultures treated with or without 500 nM of oclacitinib. The error bars represent the SD of the mean calculated from three separate and independent experiments. Statistical significance was analyzed by ANOVA with a post hoc Tukey's multiple comparison test. $^{*}p < 0.05$ and $^{**}p < 0.01$.

Furthermore, X-irradiation significantly upregulated *CCND1* and *CDK6* gene expression in HMPOS and *CCND1* gene expression in CTAC compared to no-treatment control (Figure 4B). Next, to assess the proliferative activity of each tumor cell line after exposure to X-irradiation and oclacitinib, cell cycle analysis was conducted using flow cytometry. After 24 h of X-irradiation, the G1 ratio significantly increased, and the G2 ratio significantly decreased in cells treated with oclacitinib alone compared with no-treatment control in all tumor cell lines, as well as in cells treated with X-irradiation and oclacitinib combination compared with X-irradiation alone in HMPOS and CMeC. A similar trend was observed after 48 h of X-irradiation in cells treated with X-irradiation and oclacitinib combination compared with cells treated with X-irradiation alone in all tumor cell lines. (Figure 6).

Tumor growth delay enhancement following treatment with a combination of X-irradiation and oclacitinib

To investigate the radio-sensitizing effects of oclacitinib *in vivo*, HMPOS cells were injected subcutaneously into immunodeficient nude mice, and tumor growth was assessed. The tumor volume in mice treated with X-irradiation was dramatically decreased, whereas oclacitinib alone did not decrease the tumor volume compared to that in mice without treatment (control). Tumor growth in mice treated with the X-irradiation and oclacitinib combination was obviously delayed compared to that in mice treated with X-irradiation alone (Figure 7A). The time required for a 2-fold increase in tumor volume in mice treated with X-irradiation alone was 18 days (range, 15–26 days). In contrast, in mice treated with X-irradiation and oclacitinib, it was 29 days (range, 23–60 days) after assignment (Figure 7B). The time required for a 2-fold increase in tumor volume in mice treated with X-irradiation and oclacitinib combination was significantly longer than that in mice treated with X-irradiation alone. The tumor volume did not increase even 60 days after assignment in two of the seven mice treated with the X-irradiation and oclacitinib combination.

DISCUSSION

Oclacitinib is an orally available JAK inhibitor used as a therapeutic agent for canine allergic dermatitis. In human medicine, reports have shown that inhibition of the JAK-STAT3 signaling pathway is associated with anticancer effects *in vitro* and *in vivo* through various mechanisms, including suppression of anti-apoptotic signals and establishment of immune evasion.[22,23] Although a combination of chemotherapy and oclacitinib in tumor-bearing dogs has been reported, this study aimed to assess the safety and toxicity of the combination therapy because its clinical efficacy remains elusive[26] and the anticancer effects of oclacitinib remain unclear. This study demonstrated the potential radio-sensitizing effects of oclacitinib on canine tumor cells through STAT3 activation inhibition, thereby promoting cell apoptosis and cell-cycle arrest.

It has been reported that STAT3 activation was upregulated in cells after exposure to X-irradiation in several human tumor cell lines,[27,28] but it was previously unclear whether this was also the case in canine tumors. Consistent with previous observations in human tumors, X-irradiation promoted dose- and time-dependent STAT3 activation in canine tumor cell lines. Previous studies have shown that persistent and increased induction of STAT3 activation promoted tumor migration, invasion, DNA repair, and angiogenesis, leading to tumorigenesis and tumor radio-resistance in humans.[19,27,28] Therefore, irradiation-induced STAT3 activation contributes to tumor radio-resistance in canine tumors.

A clonogenic assay was performed with various concentrations of oclacitinib alone to determine the optimal concentration for the clonogenic assay with X-irradiation. The radio-sensitivity of all tumor cell lines was significantly increased after treatment with 500 nM oclacitinib. In addition, 500 nM of oclacitinib dramatically inhibited X-irradiation-induced STAT3 activation in all the tumor cell lines.

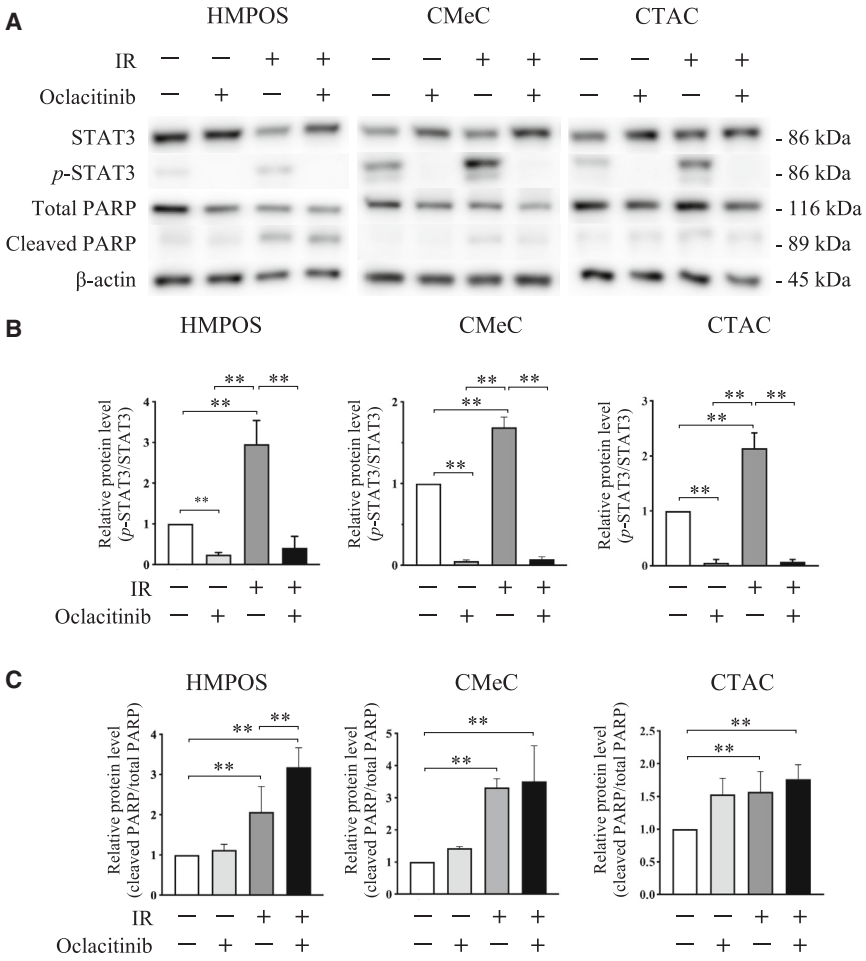

Figure 3. Effects of X-irradiation and oclacitinib on STAT3 and PARP activation in canine tumor cell lines

(A) Analysis of STAT3, phosphorylated STAT (p-STAT3), total PARP, and cleaved PARP expression in cells 24 h after 5 Gy X-irradiation (IR) with or without 500 nM of oclacitinib using western blot. β-actin served as a reference protein. (B) Comparison of the expression level of p-STAT3 relative to the corresponding total proteins. The error bars represent the SD of the mean calculated from three separate and independent experiments. Statistical significance was analyzed by Tukey's multiple comparison test. $^{**}p < 0.01$. (C) Comparison of the expression level of cleaved PARP relative to the corresponding total protein.

It has been reported that STAT3 activation in tumor cells after exposure to X-irradiation was promoted through various mechanisms, including the SPP1-JAK2-STAT3 axis, IL-6 or EGFR signaling, and the Src-STAT3 axis in human tumor cell lines.[18–20] These results show that oclacitinib can exhibit radio-sensitizing effects on tumor cells by inhibiting the JAK-STAT3 signaling pathway. The JAK-STAT3 signaling pathway may be the dominant mechanism underlying X-irradiation-induced STAT3 activation in canine tumor cells.

This study investigated the apoptotic response in tumor cells after treatment with a combination of X-irradiation and oclacitinib. Inhibition of STAT3 signaling by oclacitinib was associated with enhanced PARP activation, an apoptosis marker. In addition, the mRNA expression of anti-apoptotic genes was significantly suppressed by oclacitinib in HMPOS and CTAC but not CMeC. Consequently, the apoptotic cell rate was further increased in HMPOS and CTAC cells treated with a combination of X-irradiation and oclacitinib compared with treatment with X-irradiation and oclacitinib alone. The results of the sub-G1 phase in the cell cycle analysis further supported these findings. Survivin is one of the most important anti-apoptotic proteins, which is highly expressed in several human cancers and canine osteosarcoma.[29–31] Several studies have shown that inhibition of survivin expression enhanced apoptosis, leading to increased tumor radio-sensitivity.[32,33] Another study showed that STAT3 activation suppressed apoptosis through activation of the BCL-2 family proteins, including BCL-2, BCL-x_L, and MCL1, by regulating the expression of heat shock protein 70 and inhibiting the c-Jun N-terminal kinase pathway.[34] These findings may indicate that STAT3 signaling inhibition by oclacitinib can induce apoptosis and enhance radio-sensitivity by suppressing the anti-apoptotic mechanisms in canine tumor cells. However, this effect may vary depending on the tumor cell type.

Cell cycle progression leads to cell proliferation and is regulated by various cyclins and their CDK-binding partners.[35] It has been reported that cyclin D1 and CDK4/6 have been reported to adjust the progression of the G1 phase and that cyclin D1 was regulated by STAT3 signaling.[36–38] Previous studies have also reported that cyclin D1 promoted tumor progression and radio-resistance in various human tumor cell lines.[39,40] The results of our study showed that the expression of *CCND1* and *CDK4/6* was significantly suppressed by oclacitinib treatment. In the cell cycle analysis, X-irradiation significantly promoted cell cycle progression 48 h after X-irradiation in all tumor cell lines. Oclacitinib suppressed cell cycle progression from the G1 phase to subsequent phases 24 and 48 h after X-irradiation in all tumor cell lines. These results demonstrated that oclacitinib has a radio-sensitizing effect that inhibits cell cycle progression from the G1 phase to subsequent phases through cyclin D1 expression inhibition. In contrast, X-irradiation 24 h after treatment significantly inhibited cell cycle progression compared to that in cells without treatment in CMeC. Previous studies showed that cells have a dose-dependent

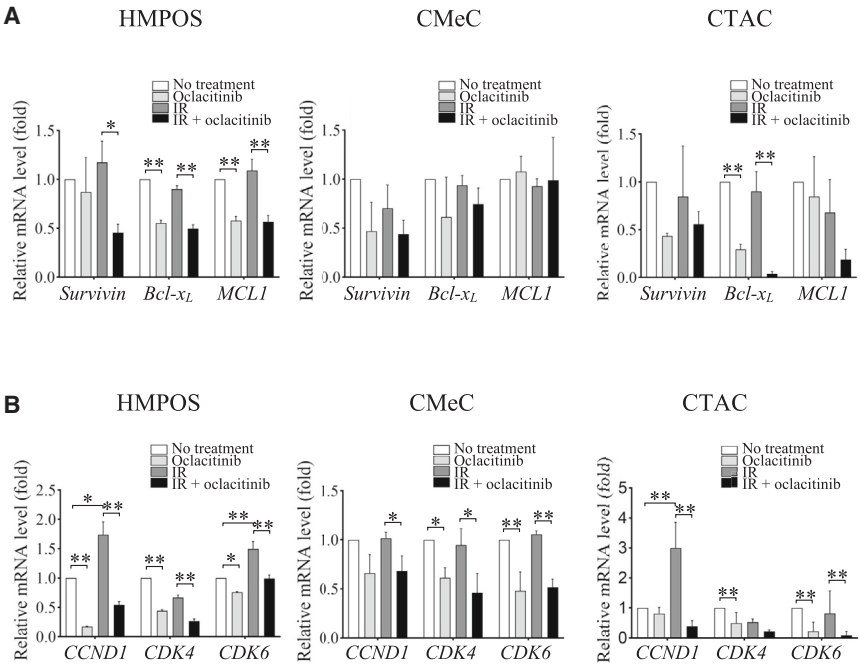

Figure 4. Gene expression in canine tumor cell lines after X-irradiation (IR) treatment with or without oclacitinib

(A) Relative mRNA levels of *survivin*, *Bcl-x_L*, and *MCL1* quantified using RT-qPCR in each condition. (B) Relative mRNA expression levels of *CCND1* and *CDK4/6* quantified using RT-qPCR in each condition. The error bars represent the SD of the mean calculated from three separate and independent experiments. Statistical significance was analyzed by Tukey's multiple comparison test. $^{*}p < 0.05$ and $^{**}p < 0.01$.

transient delay in the G1 phase of cell cycle after radiation exposure to repair critical DNA damage.[41] In the experimental protocol, 5 Gy X-irradiation was administered to cells. This dose may have led to a transient delay in the G1 phase of CMeC at 24 h after treatment.

Recently, stereotactic radiosurgery, which delivers single doses of 20 Hy or higher, has been performed for various canine tumors, including osteosarcoma and meningioma, and it has been used as an effective treatment, particularly for appendicular osteosarcoma.[42,43] Based on these findings, the radio-sensitizing effect of oclacitinib was investigated in the tumor xenograft mouse model using 20 Gy X-irradiation in a single dose. Our results showed that a combination of X-irradiation and oclacitinib significantly extended tumor regrowth delay compared to X-irradiation alone in mice transplanted with HMPOS, demonstrating the potential of oclacitinib as a radiosensitizer in canine tumors. Although no adverse effects were observed in mice after oclacitinib treatment, an X-irradiation and oclacitinib combination and higher oclacitinib concentrations (45 mg/kg) were previously used in a mouse study.[44] The oclacitinib concentrations administered in this study (10 mg/kg twice daily) were higher than those that are clinically available in dogs.[44] Considering the allometric scaling of drug doses, the oclacitinib dose of 10 mg/kg in mice is approximately equivalent to 1.8 mg/kg in dogs.[45] This dose is higher than the recommended oclacitinib dose for dogs. However, according to the manufacturer's prescribing information, administration of oclacitinib at 1.8 mg/kg twice daily in dogs resulted in only mild complications. Therefore, while this dose exceeded the recommended dose for dogs, it may be clinically achievable. Moreover, pharmacokinetic studies in dogs have shown that oral administration of clinically used doses of oclacitinib (0.4–0.6 mg/kg) resulted in a peak plasma concentration of 767.5 nM.[44]

Based on these findings, the 500 nM concentration of oclacitinib used in the *in vitro* experiments in this study is, at least transiently, pharmacologically achievable. Further analysis is required to determine whether oclacitinib can exhibit a radio-sensitizing effect in doses used in clinical settings.

In summary, oclacitinib demonstrated radiosensitizing effects in canine tumor cells *in vitro* and *in vivo* by enhancing apoptosis and inhibiting cell cycle progression. These results indicate the therapeutic potential of oclacitinib and radiotherapy for improving efficacy and outcomes in dogs.

MATERIALS AND METHODS

Cell line validation and culture conditions

A canine osteosarcoma cell line (HMPOS), which was established in our laboratory,[46] a malignant melanoma cell line (CMeC) provided by investigators at Tokyo University, Japan,[47] and a thyroid adenocarcinoma cell line (CTAC) purchased from KAC were used in this study. These cell lines have been used in previous canine tumor research[48] and were verified to be free from mycoplasma infection by PCR at the ICLAS Monitoring Center in Japan. RNA sequencing was performed to confirm their canine origin. In this study, these cell lines were cultured in RPMI-1640 medium (Thermo Fisher Scientific, Waltham, MA, USA) supplemented with 10% fetal bovine serum (FBS) (Sigma-Aldrich, St. Louis, MO, USA), 100 units/mL of penicillin G (Wako Pure Chemical Industries, Osaka, Japan), and 100 μg/mL of streptomycin (Wako Pure Chemical Industries). The cultures were maintained in a humidified atmosphere containing 5% CO_2 at 37°C.

X-ray irradiation and the reagent

Cell X-ray irradiation was administered with an XRAD iR-225 X-ray irradiator (Precision X-Ray, North Branford, CT, USA) at a dose rate of 1.37 Gy/min, operating at 200 kVp and 15 mA, with the application of a 1.0 mm aluminum filter at room temperature (RT). Oclacitinib was obtained from MedchemExpress (Monmouth Junction, NJ, USA). Oclacitinib was dissolved in dimethyl sulfoxide (DMSO; Wako Pure Chemical Industries) to prepare a 10 mM stock solution and stored at −80°C. The same volume of DMSO was added to

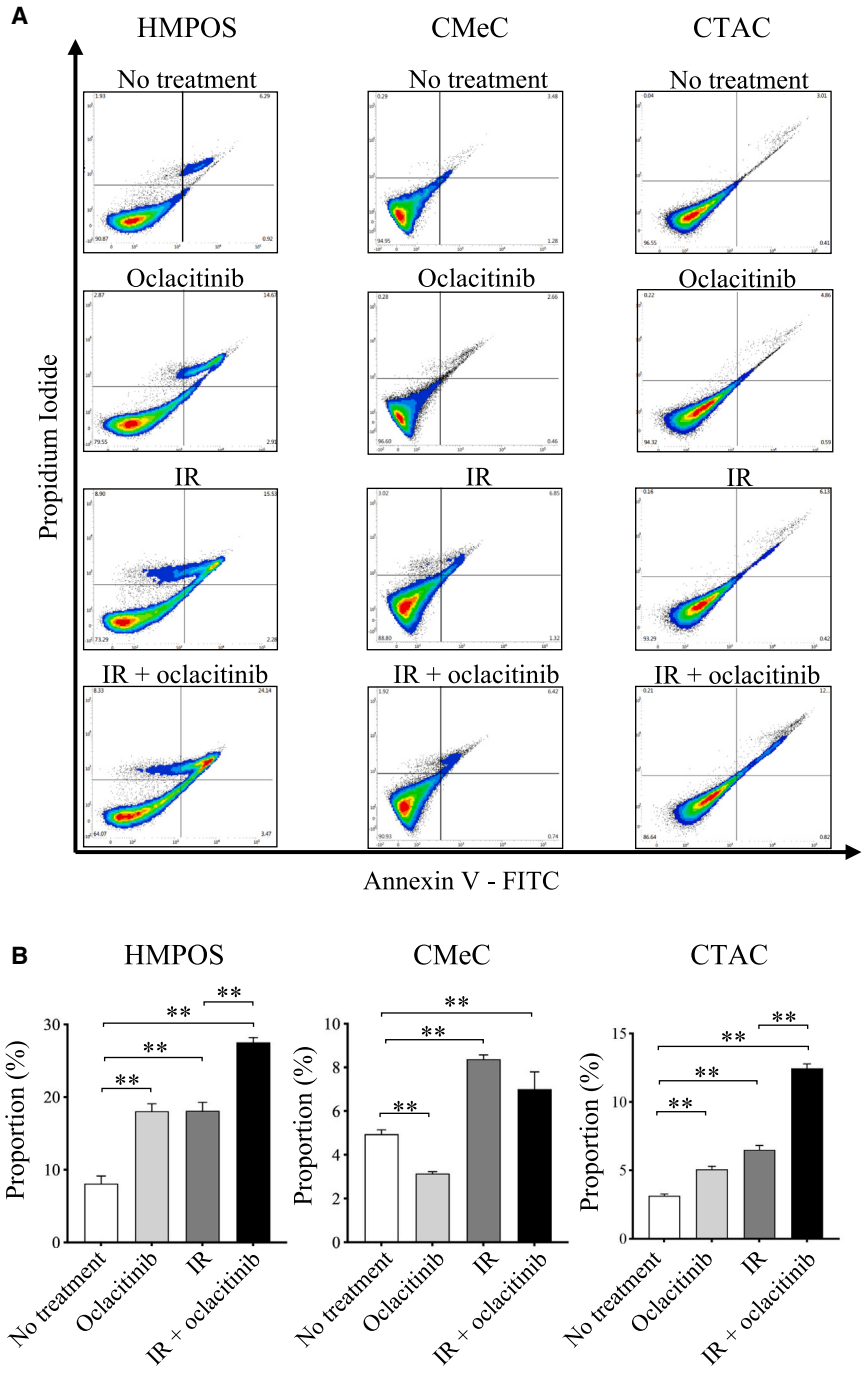

Figure 5. Effect of X-irradiation and oclacitinib on apoptosis induction in canine tumor cell lines

(A) Analysis of apoptosis in cells after exposure to 5 Gy X-irradiation (IR) with or without 500 nM of oclacitinib using flow cytometry with propidium iodide and annexin V. (B) Effects of IR and 500 nM of oclacitinib on the proportion of apoptotic cells. The error bars represent the SD of the mean calculated from three separate and independent experiments. Statistical significance was analyzed by Tukey's multiple comparison test. $^{*}p < 0.05$ and $^{**}p < 0.01$.

control wells. Under conditions involving a combination of X-irradiation and oclacitinib, each cell line (3.0×10^5 cells/well) was incubated with the specified concentrations of oclacitinib for 4 h and then exposed to 5 Gy X-irradiation.

Western blotting

Western blotting was conducted using the following antibodies: rabbit monoclonal STAT3 antibody (Cell Signaling Technology, Danvers, MA, USA), rabbit monoclonal phospho-STAT3 antibody (Cell Signaling Technology), rabbit monoclonal PARP antibody (Cell Signaling Technology), and rabbit monoclonal β-actin antibody (Cell Signaling Technology). Horseradish peroxidase (HRP)-linked anti-rabbit immunoglobulin (Ig)G (Cell Signaling Technology) was used as the secondary antibody. Each cell line (3.0×10^5 cells/well) was incubated with 500 nM of oclacitinib for 4 h and exposed to 5 Gy X-irradiation. Cells were gently washed three times with phosphate-buffered saline (PBS) and harvested at the indicated time points after X-irradiation. Cell lysis was performed using a radioimmunoprecipitation assay buffer (Sigma-Aldrich) supplemented with a protease inhibitor cocktail (Sigma-Aldrich) while maintaining samples on ice. The supernatants were collected after centrifugation at 13,000 × *g* at 4°C for 20 min. The protein concentrations were measured using a Protein Quantification Assay Kit (Macherey-Nagel, Dürren, Germany). Protein samples each of 3 μg were separated by 4%–12% sodium dodecyl sulfate-polyacrylamide gel electrophoresis, followed by transfer onto polyvinylidene difluoride membranes. The membranes were then incubated in 3% bovine serum albumin (Sigma-Aldrich) in PBS containing 0.1% Tween 20 for 1 h. Subsequently, primary antibodies against STAT3 (1:1,000), phospho-STAT3 (1:1,000), PARP (1:1,000), and β-actin (1:5,000) were added and incubated overnight at 4°C. The membranes were incubated with HRP-linked secondary antibodies (1:3,000 for STAT3, phospho-STAT3, and PARP and 1:10,000 for β-actin) for 1 h. Then, they were exposed to Western Blot Ultra-Sensitive HRP substrate (TAKARA Bio, Kusatsu, Japan) for 5 min immediately before detection. Chemiluminescence was measured using an Image Quant LAS 4000 (GE Healthcare, Buckinghamshire, UK). For the analysis of total STAT3, the pSTAT3 blots were stripped and re-probed. The intensity of each band was

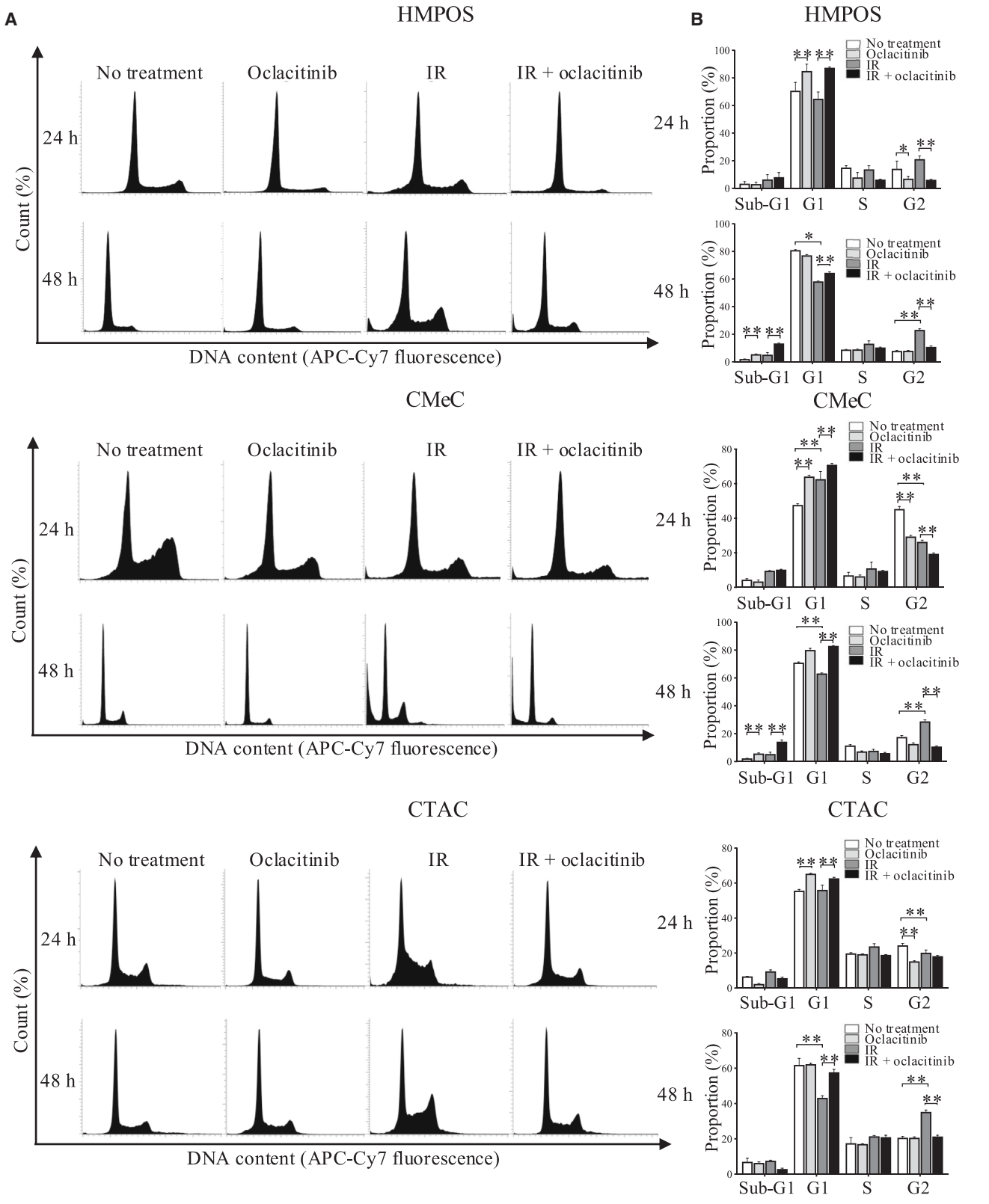

(legend on next page)

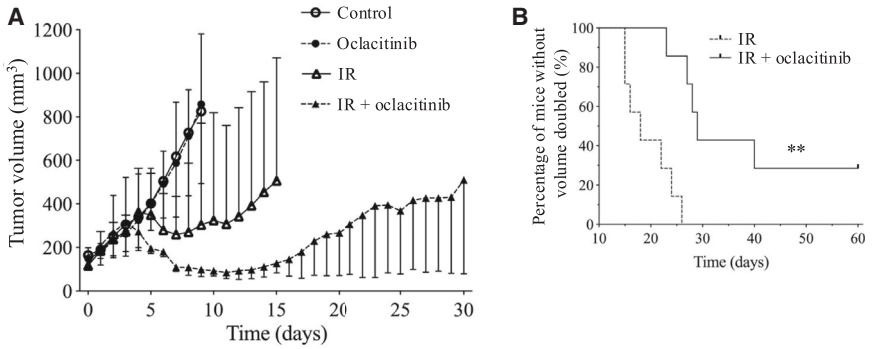

Figure 7. Tumor growth delay due to a combination of X-irradiation and oclacitinib in xenograft mice

(A) Changes in xenograft tumor volume after assignment in each group as follows: control, oclacitinib (10 mg/kg twice a day administered orally for 10 consecutive days), 20 Gy X-irradiation (IR), and IR + oclacitinib. (B) The Kaplan-Meier curves for the 2-fold increase of tumor volume after assignment. The error bars represent the range of the tumor volume for each condition. The log rank test was used to compare the percentages of mice without 2-fold increase in tumor volume. $^{*}p < 0.05$ and $^{**}p < 0.01$.

analyzed using the ImageJ software (NIH, Bethesda, MD, USA). Phospho-STAT3 and cleaved PARP levels were normalized to those of STAT3 and PARP, respectively. Protein levels in all groups were normalized to those in the control group.

Clonogenic assay

Each cell line was plated at varying concentrations in 60 mm culture dishes. Cells were cultured for 4 h with different oclacitinib concentrations, followed by exposure to varying doses of X-irradiation. Twenty-four hours after irradiation, the culture medium was replaced with fresh medium. After 7 days of incubation, the cells were fixed with ethanol and stained with Giemsa solution (Wako Pure Chemical Industries). Colonies with more than 50 cells were counted as colony-forming units. Three independent experiments were conducted, and the plating efficiency (PE) was calculated. Survival fractions were then determined, with the PE of the unirradiated control being considered for correction, and dose-response curves were generated. A linear-quadratic model was then applied to fit the survival curves, represented as $SF = (-\alpha D - \beta D^2)$, with SF denoting the surviving fraction and D representing the physical dose.

RT-qPCR

Each cell line (3.0×10^5 cells/well) was exposed to 5 Gy X-irradiation after 4 h of incubation with 500 nM oclacitinib and incubated for 24 h. Following harvesting, the cells were subjected to total RNA extraction using the TRIZol reagent (Thermo Fisher Scientific). Quantification was then performed using spectrophotometry at 260 nm. Subsequently, 500 ng of RNA was subjected to reverse transcription into cDNA using the M-MLV RT kit (Thermo Fisher Scientific) in a 20 μL reaction. Duplicate qPCR analyses were then conducted for each sample using the KAPA SYBR FAST qPCR Master Mix (2×) Kit (KAPA Biosystems, Wilmington, MA, USA). A total volume of 20 μL was prepared for each sample, which consisted of 10 μL KAPA master mix, 200 nM specific primers, and 1 μL cDNA. No template controls were performed by adding nuclease-free water. The qPCR conditions comprised an initial denaturation at 95°C for 2 min, followed by 40 cycles of denaturation at 95°C for 15 s, annealing at 60°C for 20 s, and extension at 72°C for 1 min. Relative mRNA expression was calculated using the reference gene *glyceraldehyde-3-phosphate dehydrogenase* (*GAPDH*), and quantification was performed using the delta-delta Ct method.[49] The primer sequences used in the experiments[17,50–53] are provided Table S1. All primers were previously used in canine tumor studies. Primers were designed to detect all the transcript variants. The primers for *GAPDH*, *Survivin*, *CCND1*, and *MCL1* involved spanning exon-exon junctions; the other primers could not span the junction because of the absence of exon structure information in the National Center for Biotechnology Information database (https://www.ncbi.nlm.nih.gov/). The qPCR efficiencies of these primers ranged from 97% to 102%. The specificity of the primer pairs was confirmed using a single melting peak in the melting curve analysis. Additional details of the primers used in this study are presented in Table S2.

Apoptosis analysis

Each cell line (3.0×10^5 cells/well) was incubated with 500 nM oclacitinib for 4 h before exposure to 5 Gy X-irradiation. Cells were incubated for 24 h after X-irradiation and then harvested and subjected to double staining with annexin V and propidium iodide using the Annexin V Apoptosis Detection Kit I (BD Biosciences, San Jose, CA, USA) according to the manufacturer's protocol. The apoptosis rate of cells was assessed using a BD FACS Verse Flow Cytometer (BD Biosciences). The analysis of the flow cytometry data was performed with BD FACSuite v.1.0.6 (BD Biosciences).

Cell cycle analysis

Each cell line (3.0×10^5 cells/well) was exposed to 5 Gy X-irradiation after 4 h of incubation with 500 nM oclacitinib and then incubated for 24 to 48 h. The cell lines were then harvested in 1.5 mL polypropylene tubes and subsequently stained with Cell Cycle Assay Solution Deep Red (Dojindo, Kumamoto, Japan) following the manufacturer's

Figure 6. Inhibition of the cell cycle progression from the G1 phase to subsequent phases in canine tumor cell lines due to oclacitinib treatment

(A) Analysis of DNA contents in cells treated with X-irradiation (IR) and oclacitinib using flow cytometry. (B) The cell distribution in different cell cycle phases 24 and 48 h after IR treatment with or without oclacitinib. The error bars represent the SD of the mean calculated from three separate and independent experiments. Statistical significance was analyzed by Tukey's multiple comparison test. $^{*}p < 0.05$ and $^{**}p < 0.01$.

instructions. The cells were then examined and categorized into G1, S, and G2 phases based on their DNA content using a BD FACS Verse Flow Cytometer (BD Biosciences). The analysis of the flow cytometry data was performed with BD FACSuite v.1.0.6 (BD Biosciences).

Xenograft tumor volume measurement

To assess the impact of oclacitinib on *in vivo* tumor growth, tumor growth was evaluated with a tumor xenograft mouse model. A mixture of 1.0×10^5 cells of HMPOS in 50 μL of PBS and 50 μL of Matrigel (BD Biosciences) was injected subcutaneously into the left hind legs of 7-week-old female BALB/cAJcl-nu/nu mice (CLEA Japan, Tokyo, Japan). Tumor volumes [volume = length × $(\text{width})^2/2$] and body weight were measured daily. When tumors reached 100 mm^3, mice were randomly divided into four groups: (A) control, (B) oclacitinib, (C) X-irradiation, and (D) X-irradiation and oclacitinib. The number of mice used in each group was seven. For groups B and D, oclacitinib dissolved in 0.1 mL of saline was administered orally at doses of 10 mg/kg twice a day for 10 days, whereas for groups A and C, the same volume of saline was provided as a vehicle control twice a day. The mice in groups C and D were anesthetized by isoflurane inhalation with oxygen; the body was covered with a 2-mm-thick lead sheet, and the tumor-bearing legs were locally exposed to 20 Gy X-irradiation in a single dose 3 days after starting administration of oclacitinib or saline. At the end of the assessment period, mice were humanely sacrificed by inhaling CO_2 gas. All animal experiments were performed according to the Hokkaido University Institutional Animal Care and Use Committee guidelines (approval no. 23-0122).

Statistical analysis

All results are shown as mean ± standard deviation (SD). The statistical analysis was performed with GraphPad Prism 9 software (GraphPad Software, San Diego, CA, USA). The normality of the data distribution was assessed with the Shapiro-Wilk test. For cases involving three or more groups, ANOVA followed by Tukey's multiple comparison test was conducted for data analysis. The Kaplan-Meier method was used to generate survival curves, and a statistical analysis was performed using the log rank test for the xenograft tumor volume measurement. $p < 0.05$ was considered significant.

DATA AVAILABILITY

The data that support the findings of this study are openly available in Figshare at https://doi.org/10.6084/m9.figshare.25605552.

ACKNOWLEDGMENTS

This work was supported by the Grant-in-Aid for Scientific Research (grant no. 20K06424) from the Japan Society for the Promotion of Science.

AUTHOR CONTRIBUTIONS

R.O. performed the experiments. K.H., T.D., N.M., S.K., T.S., and M.O. contributed to supervising the project. S.K., T.O., and H.Y. contributed to the interpretation of the results. K.H., T.D., N.M., and H.Y. provided the materials, reagents, and analysis tools. R.O., T.D., and N.M. prepared the manuscript. All authors reviewed and approved the manuscript.

DECLARATION OF INTERESTS

The authors declare no conflicts of interest.

SUPPLEMENTAL INFORMATION

Supplemental information can be found online at https://doi.org/10.1016/j.omton.2025.200946.

REFERENCES

1. Owen, K.L., Brockwell, N.K., and Parker, B.S. (2019). Jak-stat signaling: A double-edged sword of immune regulation and cancer progression. Cancers *11*, 2002.
2. Shen, Y., Devgan, G., Darnell, J.E., and Bromberg, J.F. (2001). Constitutively activated stat3 protects fibroblasts from serum withdrawal and UV-induced apoptosis and antagonizes the proapoptotic effects of activated Stat1. Proc. Natl. Acad. Sci. USA *98*, 1543–1548.
3. Sasse, J., Hemmann, U., Schwartz, C., Schniertshauer, U., Heesel, B., Landgraf, C., Schneider-Mergener, J., Heinrich, P.C., and Horn, F. (1997). Mutational analysis of acute-phase response factor/stat3 activation and dimerization. Mol. Cell Biol. *17*, 4677–4686.
4. Cosgrove, S.B., Wren, J.A., Cleaver, D.M., Martin, D.D., Walsh, K.F., Harfst, J.A., Follis, S.L., King, V.L., Boucher, J.F., and Stegemann, M.R. (2013). Efficacy and safety of oclacitinib for the control of pruritus and associated skin lesions in dogs with canine allergic dermatitis. Vet. Dermatol. *24*, 479-e114.
5. Cosgrove, S.B., Cleaver, D.M., King, V.L., Gilmer, A.R., Daniels, A.E., Wren, J.A., and Stegemann, M.R. (2015). Long-term compassionate use of oclacitinib in dogs with atopic and allergic skin disease: Safety, efficacy and quality of life. Vet. Dermatol. *26*, 171-e35.
6. Marsella, R., Doerr, K., Gonzales, A., Rosenkrantz, W., Schissler, J., and White, A. (2023). Oclacitinib 10 years later: lessons learned and directions for the future. J. Am. Vet. Med. Assoc. *261*, S36–S47.
7. Ryu, K., Susa, M., Choy, E., Yang, C., Hornicek, F.J., Mankin, H.J., and Duan, Z. (2010). Oleanane triterpenoid CDDO-Me induces apoptosis in multidrug resistant osteosarcoma cells through inhibition of Stat3 pathway. BMC Cancer *10*, 187.
8. Mora, L.B., Buettner, R., Seigne, J., Diaz, J., Ahmad, N., Garcia, R., Bowman, T., Falcone, R., Fairclough, R., Cantor, A., et al. (2002). Constitutive activation of stat3 in human prostate tumors and cell lines: Direct inhibition of stat3 signaling induces apoptosis of prostate cancer cells. Cancer Res. *62*, 6659–6666.
9. Banerjee, K., and Resat, H. (2016). Constitutive activation of STAT3 in breast cancer cells: A review. Int. J. Cancer *138*, 2570–2578.
10. Wang, X., Goldstein, D., Crowe, P.J., and Yang, J.L. (2014). Impact of STAT3 inhibition on survival of osteosarcoma cell lines. Anticancer. Res. *34*, 6537–6545.
11. Kulesza, D.W., Ramji, K., Maleszewska, M., Mieczkowski, J., Dabrowski, M., Chouaib, S., and Kaminska, B. (2019). Search for novel STAT3-dependent genes reveals SERPINA3 as a new STAT3 target that regulates invasion of human melanoma cells. Lab. Invest. *99*, 1607–1621.
12. Thomas, S.J., Snowden, J.A., Zeidler, M.P., and Danson, S.J. (2015). The role of JAK/STAT signalling in the pathogenesis, prognosis and treatment of solid tumours. Br. J. Cancer *113*, 365–371.
13. Yu, H., Lee, H., Herrmann, A., Buettner, R., and Jove, R. (2014). Revisiting STAT3 signalling in cancer: New and unexpected biological functions. Nat. Rev. Cancer. *14*, 736–746.
14. Liu, I.L., Chung, T.F., Huang, W.H., Hsu, C.H., Liu, C.C., Chiu, Y.H., Huang, K.C., Liao, A.T.C., and Lin, C.S. (2021). Kynurenine 3-monooxygenase (KMO), and signal transducer and activator of transcription 3 (STAT3) expression is involved in tumour proliferation and predicts poor survival in canine melanoma. Vet. Comp. Oncol. *19*, 79–91.
15. Bid, H.K., Oswald, D., Li, C., London, C.A., Lin, J., and Houghton, P.J. (2012). Anti-angiogenic activity of a small molecule STAT3 inhibitor LLL12. PLoS One *7*, e35513.
16. Assumpção, A.L.F.V., Jark, P.C., Hong, C.C., Lu, Z., Ruetten, H.M., Heaton, C.M., Pinkerton, M.E., and Pan, X. (2018). STAT3 expression and activity are up-regulated in diffuse large B cell lymphoma of dogs. J. Vet. Intern. Med. *32*, 361–369.

17. Couto, J.I., Bear, M.D., Lin, J., Pennel, M., Kulp, S.K., Kisseberth, W.C., and London, C.A. (2012). Biologic activity of the novel small molecule STAT3 inhibitor LLL12 against canine osteosarcoma cell lines. BMC Vet. Res. *8*, 244.

18. Wang, M., Sun, X., Xin, H., Wen, Z., and Cheng, Y. (2022). SPP1 promotes radiation resistance through JAK2/STAT3 pathway in esophageal carcinoma. Cancer Med. *11*, 4526–4543.

19. Gao, L., Li, F.S., Chen, X.H., Liu, Q.W., Feng, J.B., Liu, Q.J., and Su, X. (2014). Radiation induces phosphorylation of STAT3 in a dose- and time-dependent manner. Asian Pac. J. Cancer Prev. *15*, 6161–6164.

20. Singh-Gupta, V., Zhang, H., Banerjee, S., Kong, D., Raffoul, J.J., Sarkar, F.H., and Hillman, G.G. (2009). Radiation-induced HIF-1α cell survival pathway is inhibited by soy isoflavones in prostate cancer cells. Int. J. Cancer *124*, 1675–1684.

21. Yan, S., Li, Z., and Thiele, C.J. (2013). Inhibition of STAT3 with orally active JAK inhibitor, AZD1480, decreases tumor growth in neuroblastoma and pediatric sarcomas *in vitro* and *in vivo*. Oncotarget *4*, 433–445.

22. Pitroda, S.P., Stack, M.E., Liu, G.F., Song, S.S., Chen, L., Liang, H., Parekh, A.D., Huang, X., Roach, P., Posner, M.C., et al. (2018). JAK2 inhibitor sar302503 abrogates pd-l1 expression and targets therapy-resistant non–small cell lung cancers. Mol. Cancer Therapeut. *17*, 732–739.

23. Sun, Y., Moretti, L., Giacalone, N.J., Schleicher, S., Speirs, C.K., Carbone, D.P., and Lu, B. (2011). Inhibition of JAK2 signaling by TG101209 enhances radiotherapy in lung cancer models. J. Thorac. Oncol. *6*, 699–706.

24. Zhang, Q., Zhou, X.M., Wei, S.Z., Cui, D.S., Deng, K.L., Liang, G., Luo, Y., Luo, B., and Liang, X.J. (2022). STAT3 as a target for sensitizing prostate cancer cells to irradiation. J. Radiat. Res. *63*, 174–182.

25. Lu, L., Dong, J., Wang, L., Xia, Q., Zhang, D., Kim, H., Yin, T., Fan, S., and Shen, Q. (2018). Activation of STAT3 and Bcl-2 and reduction of reactive oxygen species (ROS) promote radioresistance in breast cancer and overcome of radioresistance with niclosamide. Oncogene *37*, 5292–5304.

26. Barrett, L.E., Gardner, H.L., Barber, L.G., Sadowski, A., and London, C.A. (2019). Safety and toxicity of combined oclacitinib and carboplatin or doxorubicin in dogs with solid tumors: A pilot study. BMC Vet. Res. *15*, 291.

27. Lau, J., Ilkhanizadeh, S., Wang, S., Miroshnikova, Y.A., Salvatierra, N.A., Wong, R.A., Schmidt, C., Weaver, V.M., Weiss, W.A., and Persson, A.I. (2015). STAT3 blockade inhibits radiation-induced malignant progression in glioma. Cancer Res. *75*, 4302–4311.

28. Wang, F., Ma, X., Mao, G., Zhang, X., and Kong, Z. (2021). STAT3 enhances radiation-induced tumor migration, invasion and stem-like properties of bladder cancer. Mol. Med. Rep. *23*, 87.

29. Fossey, S.L., Liao, A.T., Mccleese, J.K., Bear, M.D., Lin, J., Li, P.K., Kisseberth, W.C., and London, C.A. (2009). Characterization of STAT3 activation and expression in canine and human osteosarcoma. BMC Cancer *9*, 81.

30. Kanda, N., Seno, H., Konda, Y., Marusawa, H., Kanai, M., Nakajima, T., Kawashima, T., Nanakin, A., Sawabu, T., Uenoyama, Y., et al. (2004). STAT3 is constitutively activated and supports cell survival in association with survivin expression in gastric cancer cells. Oncogene *23*, 4921–4929.

31. Gritsko, T., Williams, A., Turkson, J., Kaneko, S., Bowman, T., Huang, M., Nam, S., Eweis, I., Diaz, N., Sullivan, D., et al. (2006). Persistent activation of stat3 signaling induces survivin gene expression and confers resistance to apoptosis in human breast cancer cells. Clin. Cancer Res. *12*, 11–19.

32. Lu, B., Mu, Y., Cao, C., Zeng, F., Schneider, S., Tan, J., Price, J., Chen, J., Freeman, M., and Hallahan, D.E. (2004). Survivin as a therapeutic target for radiation sensitization in lung cancer. Cancer Res. *64*, 2840–2845.

33. Iwasa, T., Okamoto, I., Suzuki, M., Nakahara, T., Yamanaka, K., Hatashita, E., Yamada, Y., Fukuoka, M., Ono, K., and Nakagawa, K. (2008). Radiosensitizing effect of YM155, a novel small-molecule survivin suppressant, in non-small cell lung cancer cell lines. Clin. Cancer Res. *14*, 6496–6504.

34. Zorzi, E., and Bonvini, P. (2011). Inducible Hsp70 in the regulation of cancer cell survival: Analysis of chaperone induction, expression and activity. Cancer *3*, 3921–3956.

35. Bertoli, C., Skotheim, J.M., and De Bruin, R.A.M. (2013). Control of cell cycle transcription during G1 and S phases. Nat. Rev. Mol. Cell Biol. *14*, 518–528.

36. Pan, L., Zhang, R., Ma, L., Pierson, C.R., Finlay, J.L., Li, C., and Lin, J. (2021). STAT3 inhibitor in combination with irradiation significantly inhibits cell viability, cell migration, invasion and tumorsphere growth of human medulloblastoma cells. Cancer. Biol. Ther. *22*, 430–439.

37. Ma, J.H., Qin, L., and Li, X. (2020). Role of STAT3 signaling pathway in breast cancer. Cell Commun. Signal. *18*, 33.

38. Hydbring, P., Malumbres, M., and Sicinski, P. (2016). Non-canonical functions of cell cycle cyclins and cyclin-dependent kinases. Nat. Rev. Mol. Cell Biol. *17*, 280–292.

39. Im, H., Lee, J., Lee, H.J., Kim, D.Y., Kim, E.J., and Yi, J.Y. (2023). Cyclin D1 promotes radioresistance through regulation of RAD51 in melanoma. Exp. Dermatol. *32*, 1706–1716.

40. Choi, C., Park, S., Cho, W.K., and Choi, D.H. (2019). Cyclin D1 is associated with radiosensitivity of triple-negative breast cancer cells to proton beam irradiation. Int. J. Mol. Sci. *20*, 4943.

41. Licursi, V., Anzellotti, S., Favaro, J., Sineri, S., Carucci, N., Cundari, E., Fiore, M., Guarguaglini, G., Pippa, S., Nisi, P.S., et al. (2020). X-ray irradiated cultures of mouse cortical neural stem/progenitor cells recover cell viability and proliferation with dose-dependent kinetics. Sci. Rep. *10*, 6562.

42. Kubicek, L., Vanderhart, D., Wirth, K., An, Q., Chang, M., Farese, J., Bova, F., Sudhyadhom, A., Kow, K., Bacon, N.J., and Milner, R. (2016). Association between computed tomographic characteristics and fractures following stereotactic radiosurgery in dogs with appendicular osteosarcoma. Vet. Radiol. Ultrasound *57*, 321–330.

43. Kelsey, K.L., Gieger, T.L., and Nolan, M.W. (2018). Single fraction stereotactic radiation therapy (stereotactic radiosurgery) is a feasible method for treating intracranial meningiomas in dogs. Vet. Radiol. Ultrasound *59*, 632–638.

44. Collard, W.T., Hummel, B.D., Fielder, A.F., King, V.L., Boucher, J.F., Mullins, M.A., Malpas, P.B., and Stegemann, M.R. (2014). The pharmacokinetics of oclacitinib maleate, a Janus kinase inhibitor, in the dog. J. Vet. Pharmacol. Therapeut. *37*, 279–285.

45. Sharma, V., and Mcneill, J.H. (2009). To scale or not to scale: the principles of dose extrapolation. Br. J. Pharmacol. *157*, 907–921.

46. Barroga, E.F., Kadosawa, T., Okumura, M., and Fujinaga, T. (1999). Establishment and characterization of the growth and pulmonary metastasis of a highly lung metastasizing cell line from canine osteosarcoma in nude mice. J. Vet. Med. Sci. *61*, 361–367.

47. Inoue, K., Ohashi, E., Kadosawa, T., Hong, S.H., Matsunaga, S., Mochizuki, M., Nishimura, R., and Sasaki, N. (2004). Establishment and characterization of four canine melanoma cell lines. J. Vet. Med. Sci. *66*, 1437–1440.

48. Owaki, R., Deguchi, T., Konnai, S., Maekawa, N., Okagawa, T., Hosoya, K., Kim, S., Sunaga, T., and Okumura, M. (2023). Regulation of programmed death ligand 1 expression by interferon-γ and tumour necrosis factor-α in canine tumour cell lines. Vet. Comp. Oncol. *21*, 279–290.

49. De Bruin, T., De Rooster, H., Van Bree, H., and Cox, E. (2005). Interleukin-8 mRNA expression in synovial fluid of canine stifle joints with osteoarthritis. Vet. Immunol. Immunopathol. *108*, 387–397.

50. Sano, J., Oguma, K., Kano, R., Yazawa, M., Tsujimoto, H., and Hasegawa, A. (2005). High expression of Bcl-xL in delayed apoptosis of canine neutrophils induced by lipopolysaccharide. Res. Vet. Sci. *78*, 183–187.

51. Wang, Y., Mwale, C., Akaraphutiporn, E., Kim, S., Sunaga, T., and Okumura, M. (2023). Sulfate level relied effects of pentosan polysulfate sodium on inhibiting the proliferationof canine articular chondrocytes by targeting PI3K/Akt pathway. Jpn. J. Vet. Res. *71*, 35–47.

52. Akaraphutiporn, E., Bwalya, E.C., Kim, S., Sunaga, T., Echigo, R., and Okumura, M. (2020). Effects of pentosan polysulfate on cell proliferation, cell cycle progression and cyclin-dependent kinases expression in canine articular chondrocytes. J. Vet. Med. Sci. *82*, 1209–1218.

53. Bwalya, E.C., Kim, S., Fang, J., Wijekoon, H.M.S., Hosoya, K., and Okumura, M. (2017). Pentosan polysulfate inhibits IL-1β-induced iNOS, c-Jun and HIF-1α upregulation in canine articular chondrocytes. PLoS One *12*, e0177144.